

Subdiffraction-Limit Two-Photon Fluorescence Microscopy for GFP-Tagged Cell Imaging

Qifeng Li, Sherry S. H. Wu, and Keng C. Chou*

Department of Chemistry, University of British Columbia, Vancouver, British Columbia, Canada

ABSTRACT We report applications of two-photon excitation fluorescence (2PEF) microscopy with subdiffraction-limit resolution for green-fluorescent-protein-tagged cell imaging. The microscope integrates 2PEF microscopy and stimulated emission depletion microscopy in one microscope that has the benefits of both techniques: intrinsic three-dimensional resolution, confined photobleaching, and subdiffraction-limit resolution. The subdiffraction-limit resolution was demonstrated by resolving green-fluorescent-protein-tagged caveolar vesicles located within a distance shorter than the diffraction limit of a regular 2PEF microscope, which is ~250 nm even with the best optics. The full width at half-maximum of the effective point-spread function for the 2PEF microscope was estimated to be ~54 nm.

INTRODUCTION

Far-field fluorescent microscopy is widely used in molecular cell biology for noninvasive and high-specificity imaging. Over the past century, the resolution of far-field optical microscopes has been limited by the well known diffraction limit, which limits the resolution to $\lambda/2 \times \text{NA}$, where λ and NA denote the wavelength of light and the numerical aperture of the objective lens, respectively. Modern immersion microscopes have been improving the resolution by using objective lenses with high NA, but the improvement in the NA has been limited by the availability of transparent materials. With all these limitations, the resolution of a far-field fluorescent microscope is typically in the range 200–300 nm, which makes it unable to resolve many fine structures in a cell. Recently, significant efforts have been made to develop far-field optical microscopy with subdiffraction-limit resolution, such as stimulated emission depletion (STED) (1), photoactivated localization microscopy (2,3), and stochastic optical reconstruction microscopy (4). These developments have achieved lateral resolution of tens of nanometers and allowed researchers to observe biological structures with unprecedented resolution (5–8).

Two-photon excitation fluorescence (2PEF) microscopy is a popular alternative to one-photon excitation fluorescence microscopy (9). It provides intrinsic three-dimensional resolution and often reduces overall phototoxicity, because the excitation and photobleaching are confined to the focal spot. For these reasons, 2PEF microscopy is particularly useful for optical imaging and manipulations within a localized region. Recently, a 2PEF microscope combined with STED was demonstrated by Moneron and Hell (10). STED microscopy is a powerful approach to achieve a subdiffraction-limit resolution (11,12). In a STED microscope, the

size of the effective fluorescence spot was reduced by depleting the spontaneous fluorescence emission in the outer regions of the excitation area using stimulated emission (1,13). In this approach, the decrease in the size of the fluorescence spot is equivalent to an increase in the resolution. Previous work by Moneron and Hell was carried out using fluorescent dyes. In this work, we study the application of a 2PEF-STED microscope for imaging green fluorescent protein (GFP). Although GFP does not have the best brightness or photostability compared to many dyes (14), it is a particularly important fluorescent label for biological imaging, because the GFP gene can be fused to the gene of interest and expressed within the living cells (15,16). In addition, GFP is noninvasive, whereas many fluorescent dyes are toxic. By combining 2PEF and STED microscopy techniques, we have demonstrated a subdiffraction-limit resolution and resolved single GFP-tagged caveolae, which function as transported vesicles in many cell physiological processes, including endocytic and exocytic pathways, signal transduction, and lipid regulation (17).

MATERIALS AND METHODS

2PEF-STED microscopy

The layout of the 2PEF-STED microscope is shown in Fig. 1 *a*. Two-photon excitation was carried out using a 130-fs Ti:sapphire laser (MIRA 900, Coherent, Santa Clara, CA) with a wavelength of 850 nm and a repetition rate of 76 MHz. The depletion beam at 580 nm was obtained by pumping a home-made intracavity-frequency-doubled optical parametric oscillator with a second Ti:sapphire laser. The 580-nm beam was coupled into a 40-meter polarization-maintaining single-mode fiber (460HP, Thorlabs, North Newton, NJ) to stretch the pulse duration from 130 fs to 200 ps. The doughnut-shaped focal intensity profile of the depletion beam (Fig. 1 *b*), was obtained using a spiral phase plate (RPC Photonics, Rochester, NY), which was proposed by Torok, et al. (13) and used by Hell and his co-workers for STED microscopy (1,18). Fig. 1, *b* and *c*, shows the intensity profiles of the depletion and excitation beams, respectively, recorded by the scattering light from a 100-nm gold particle (C-Au-0.100, Microspheres-Nanospheres, Cold Spring, NY). The two beams were then combined using a dichroic mirror

Submitted July 24, 2009, and accepted for publication September 16, 2009.

Qifeng Li and Sherry S. H. Wu contributed equally to this work.

*Correspondence: kcchou@chem.ubc.ca

Editor: Levi A. Gheber.

© 2009 by the Biophysical Society
0006-3495/09/12/3224/5 \$2.00

doi: 10.1016/j.bpj.2009.09.038

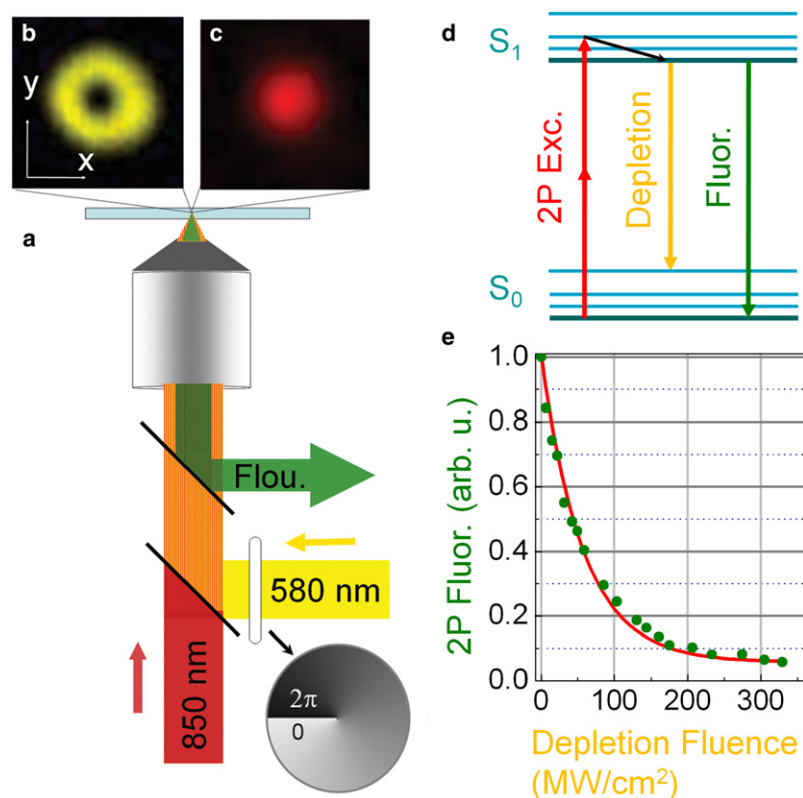


FIGURE 1 (a) Experimental setup for 2PEF-STED microscopy. (b) The doughnut-shaped intensity profile of the 580-nm depletion beam obtained using the spiral phase plate shown in *a*. (c) Gaussian intensity profile of the two-photon excitation beam at 850 nm. The intensity profiles were recorded by the scattering light from a 100-nm gold particle. (d) Energy diagram for the 2PEF-STED microscopy. (e) Measured 2P fluorescence depletion efficiency for GFP.

(FF665-Di01-25×36, Semrock, Rochester, NY) before entering the objective lens (100×, NA 1.4 oil, HCX PL APO CS, Leica, Germany). The two-photon excitation spot (Fig. 1 *c*) was then positioned at the center of the doughnut-shaped depletion beam (Fig. 1 *b*). Two laser beams were synchronized and overlapped in time to maximize the depletion of the 2PEF. The 2PEF was then collected with a lens, coupled to a 62-μm optical fiber, and detected by a photomultiplier tube (R4220P, Hamamatsu, Japan) and a pulse counter (National Instruments, Austin, TX). All images were obtained with the samples mounted on a three-dimensional piezo-scanning stage (Nano-LP200, Mad City Labs, Madison, WI). The laser beams were fixed, while the piezo-scanning stage was scanned at a speed of 5 ms/pixel.

Cell culture and transfection

Chinese hamster ovary (CHO) cells were cultured in Alpha-MEM (Invitrogen Life Technologies, Carlsbad, CA) containing 10% FBS and 2 mM L-glutamine at 37°C in a 5% CO₂ incubator. To establish a stable cell line, CHO cells were transfected with Plasmid Cav1-GFP (Addgene plasmid 14433) using lipofectamine 2000 (Invitrogen) according to manufacturer's instruction, and cultured in the presence of 1 mg/ml of G418 (Invitrogen) for 3 weeks. The CHO cells expressing Cav1-GFP were fixed in 2% paraformaldehyde/PBS for 10 min, washed with 1× PBS, and mounted in glycerol/PBS.

RESULTS AND DISCUSSION

Fig. 1 *d* shows a typical two-photon (2P) excitation energy diagram. The 2P excitation from the ground S_0 state is achieved via simultaneous absorption of two near-infrared photons. The excitation then quickly relaxes to lower vibrational levels in the S_1 . Without an external field, the population in S_1 decays to the ground-state S_0 via spontaneous emission. There are many GFP derivatives (19). The

enhanced green fluorescent protein (EGFP), which was used in this study, is one of the most used mutants, because it is brighter than the wild-type GFP (20). The absorption and emission spectra of EGFP peak at 488 nm and 508 nm, respectively. The 2P excitation mechanism for GFP remains as an active research area and is not yet fully understood. An additional peak has been reported near 440 nm in a two-photon excitation process, but not observed in one-photon excitation processes (21). Recently, it was proposed that EGFP has a hidden electronic excited state (S_2) for 2P excitations near the lowest excited singlet (S_1) (22).

To carry out 2PEF-STED microscopy for GFP-tagged cell imaging, it is critical to verify that the STED technique is effective for 2P-excited GFP. In STED microscopy, the spatial extent of the fluorescence spot given by the excitation profile (Fig. 1 *c*) is reduced by inhibiting the spontaneous fluorescence emission in the outer regions using stimulated emission (1,18,23). To reduce the excited-state population and the spontaneous fluorescence emission, a laser pulse is applied to stimulate transitions to the upper vibrational levels of S_0 , as indicated by the yellow arrow in Fig. 1 *d*. The wavelength of this depletion beam must be sufficiently longer than that for the single-photon absorption to avoid exciting the fluorescent molecules. Previously, a 50% depletion of fluorescence from 2P-excited fluorescein in ethylene glycol and methanol has been demonstrated (24), and a depletion of 70% was shown using synthesized conjugated fluorophores OM62C (25) designed for enhanced 2P absorption

cross section (26). In these 2P excitation studies, depletion beams with a pulse duration of ~ 2 ps were used, but it has been shown by Hell and his co-workers that a depletion beam with a pulse duration of >50 ps is beneficial (10,27). A depletion period much longer than the vibrational relaxation time in S_0 (typically subpicosecond) also allows the depletion pulse to stimulate the excited molecules in S_1 into a vibrational state in S_0 that is mostly empty. Fig. 1 *e* shows the 2PEF intensity from GFP as a function of the fluence of the depletion beam at 580 nm with a pulse duration of 200 ps. With a fluence of 300 MW/cm², nearly 95% of the fluorescence can be depressed. The 580-nm beam also excites a small portion of GFP. However, the fluorescence excited by the 580-nm beam has been mostly excluded from the detection system by using an optical fiber. When the 2PEF was coupled to the fiber, the core diameter of the fiber (62.5 μ m) was carefully chosen to be ~ 0.6 Airy units. In this case, the fluorescence from the doughnut-shaped depletion beam was mostly filtered by the fiber because the intensity of the depletion beam was nearly zero at the center of the doughnut.

Fig. 2, *a* and *b*, shows EGFP-tagged caveolin 1 (Cav1-GFP) in CHO cells imaged by regular 2PEF microscope and by the 2PEF-STED microscope, respectively. The regular 2PEF image was taken with an excitation beam of 1.8 mW at 850 nm. The 2PEF-STED image was obtained with an excitation beam of 2.7 mW at 850 nm and a depletion beam of 4.4 mW at 580 nm. The photon count in the 2PEF-STED was significantly lower than that in the 2PEF image,

because the intensity of 2P fluorescence decreased as the size of the fluorescent spot was reduced by the depletion beam. A higher 2P excitation power was used to partially compensate for the fluorescence signal reduction, but overall, a trade-off exists between the fluorescence intensity and the resolution: a better resolution can be obtained with a smaller fluorescent spot, but a smaller fluorescent spot produces less fluorescence. Because of the lower photon count, images obtained by STED microscopy are often smoothed or restored by various filters to remove noise (18,28–30). Fig. 2, *c* and *d*, are the same images as in Fig. 2, *a* and *b*, respectively, after image restoration with the Tikhonov-Miller filter (16,31). Fluorescence spots of various sizes can be seen in Fig. 2 because caveolins exist in different cellular structures in the cytoplasm. Caveolin 1 is the major structural protein on the surface of caveolae (17). Cav1-GFP has been shown to exist in caveolae, protein-lipid complexes, and larger cellular structures such as the Golgi complex, caveosomes, and early endosomes (32). The small Cav1-GFP domains are presumed to be caveolar vesicles or protein-lipid chaperon complexes, which have diameters of 50–100 nm under an electron microscope (33).

Fig. 2, *e* and *f*, are magnified views of the marked areas in Fig. 2, *c* and *d*, respectively. The regular 2PEF microscope has a diffraction-limited excitation spot with a full width at half-maximum (FWHM) of ~ 250 nm. Consequently, all features observed in the regular 2PEF images (Fig. 2 *c* and *e*) have FWHMs >250 nm because of the diffraction limit.

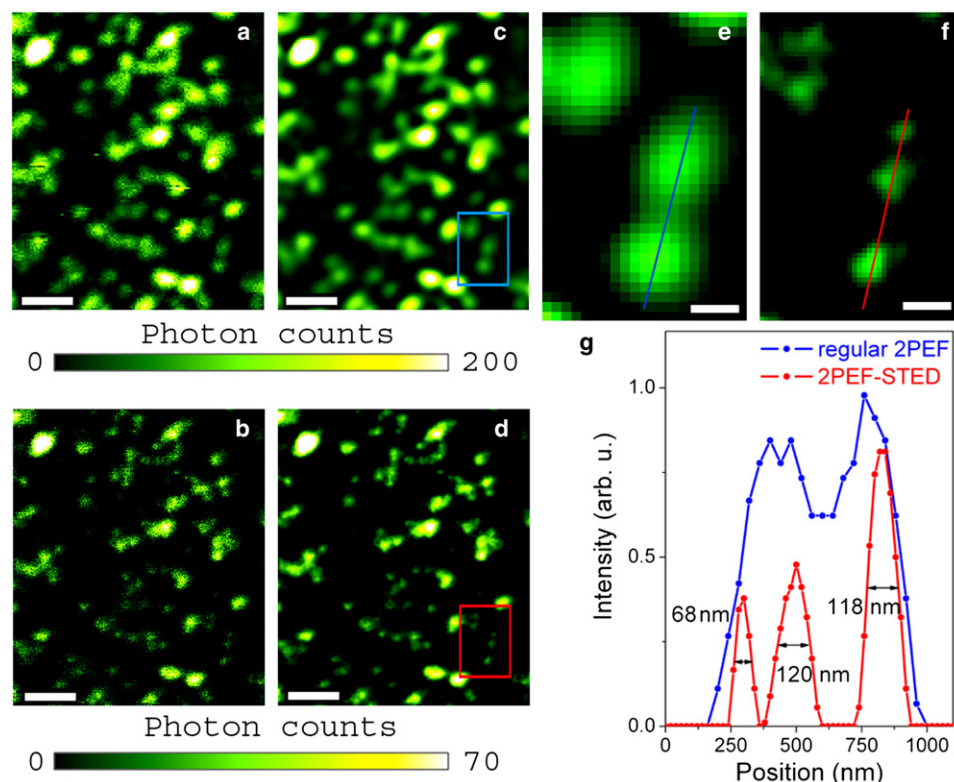


FIGURE 2 EGFP-tagged caveolin in a CHO cell imaged using (*a*) a regular 2PEF microscope and (*b*) the 2PEF-STED microscope described in this study. (*c*) Regular 2PEF and (*d*) 2PEF-STED images after image restoration by the Tikhonov-Miller filter. (*e*) Magnified view of the marked area for the regular 2PEF image in *c*. (*f*) Magnified view of the same marked area for the 2PEF-STED image in *d*. (*g*) Intensity profiles of the regular 2PEF and 2PEF-STED images, as indicated in *e* and *f*. The scale bars, 1 μ m (*a–d*) and 200 nm (*e* and *f*). Pixel sizes, 40 nm (*e*) and 20 nm (*f*).

With the 2PEF-STED microscope; however, we could distinguish two caveolar vesicles located within a distance smaller than the 250-nm diffraction limit, as shown in Fig. 2 *f* and its profile in Fig. 2 *g*. A single caveolar vesicle with a FWHM of 68 nm was observed.

The FWHM of the effective point-spread function (PSF) for the 2PEF-STED microscope can be estimated using the size of the caveolar vesicles measured by electron microscopy, which have diameters in the range 50–100 nm (33). As described previously, the effective fluorescence spot of STED microscopy was reduced by depleting the spontaneous fluorescence emission in the outer regions using stimulated emission. The size of the subdiffraction-limit fluorescent spot can be regarded as the effective PSF for the STED microscopy (12,29). In general, the measured image profile $h_{\text{imag}}(\vec{r})$ is a convolution of the effective PSF $h_{\text{eff}}(\vec{r})$ and the profile of the object $h_{\text{obj}}(\vec{r})$:

$$h_{\text{imag}}(\vec{r}) = h_{\text{eff}}(\vec{r}) \otimes h_{\text{obj}}(\vec{r}). \quad (1)$$

In this study, an optical fiber was used to couple the fluorescence signal into the detector. Therefore, the fluorescence profile, $h_{\text{fluo}}(\vec{r})$, given by the 2P excitation at the entrance of the fiber, and the size of the fiber aperture $A(\vec{r})$ need to be taken into account, and $h_{\text{imag}}(\vec{r})$ can be written as (29)

$$h_{\text{imag}}(\vec{r}) = h_{\text{eff}}(\vec{r}) \otimes h_{\text{obj}}(\vec{r}) (h_{\text{fluo}}(\vec{r}) \otimes A(\vec{r}')) \quad (2)$$

It has been shown that the effective PSF $h_{\text{eff}}(\vec{r})$ for STED microscopy can be expressed as (7,12,29)

$$h_{\text{eff}}(\vec{r}) = h_{\text{fluo}}(\vec{r}) \exp(-h_{\text{STED}}(\vec{r})\zeta), \quad (3)$$

where $h_{\text{STED}}(\vec{r})$ is the depletion STED beam intensity profile shown in Fig. 1 *b*, and $\zeta = I/I_s$ gives the “saturation factor” of the depletion, where I denotes the peak intensity of the STED beam and I_s the characteristic intensity at which the fluorescence intensity is reduced to half (7). Assuming the smallest vesicle has a diameter of 50 nm, with a uniform intensity profile $h_{\text{obj}}(\vec{r})$, as shown in Fig. 3 *a*, an image profile with a FWHM of 68 nm (Fig. 3 *c* and 3 *g*) can be obtained using an effective PSF with a FWHM of 54 nm, as shown in Fig. 3 *b*. Although there is no theoretical limit on the resolution of STED microscopy, there is a trade-off between the resolution and photobleaching. The 2PEF-STED images shown in this study were obtained with 4.4 mW of depletion beam. Roughly 10–20% of the GFPs were bleached after one scan. The photobleaching can be reduced with a decreased depletion beam power and lower resolution. Experimentally, a resolution of ~100 nm can be easily achieved with a depletion power of 1–2 mW.

CONCLUSION

A 2PEF microscope with subdiffraction-limit resolution for GFP-tagged cell imaging was achieved using stimulated-emission depletion. The subdiffraction-limit resolution was

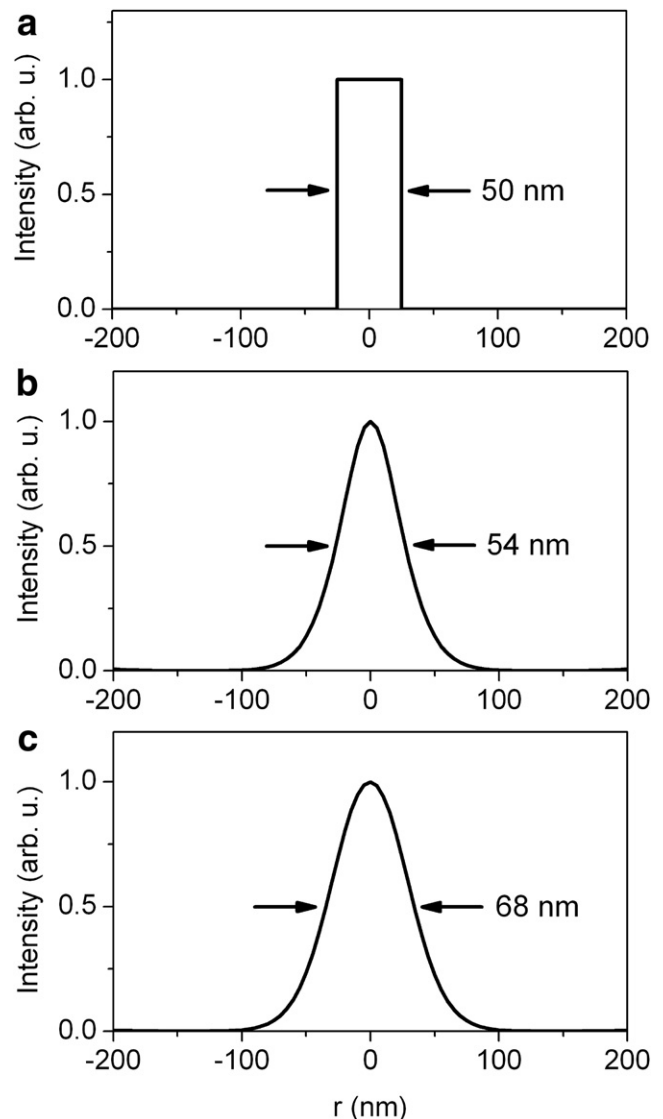


FIGURE 3 Estimation of the effective PSF for the 2PEF-STED microscope. (a) A vesicle profile with a diameter of 50 nm. (b) The effective PSF with a FWHM of 54 nm. (c) Image profile obtained via the convolution of *a* and *b*.

demonstrated by distinguishing GFP-tagged caveolar vesicles located within a distance shorter than the diffraction limit of a regular 2PEF microscope. The FWHM of the effective PSF of the 2PEF-STED microscope was estimated to be ~54 nm.

We thank Professor Ari Helenius for kindly providing the Cav1-GFP construct.

This work was supported in part by the Canada Foundation for Innovation and the Natural Sciences and Engineering Research Council of Canada.

REFERENCES

- Willig, K. I., S. O. Rizzoli, V. Westphal, R. Jahn, and S. W. Hell. 2006. STED microscopy reveals that synaptotagmin remains clustered after synaptic vesicle exocytosis. *Nature*. 440:935–939.

2. Betzig, E., G. H. Patterson, R. Sougrat, O. W. Lindwasser, S. Olenych, et al. 2006. Imaging intracellular fluorescent proteins at nanometer resolution. *Science*. 313:1642–1645.
3. Hess, S. T., T. P. K. Girirajan, and M. D. Mason. 2006. Ultra-high resolution imaging by fluorescence photoactivation localization microscopy. *Biophys. J.* 91:4258–4272.
4. Rust, M. J., M. Bates, and X. W. Zhuang. 2006. Sub-diffraction-limit imaging by stochastic optical reconstruction microscopy (STORM). *Nat. Methods*. 3:793–795.
5. Kittel, R. J., C. Wichmann, T. M. Rasse, W. Fouquet, M. Schmidt, et al. 2006. Bruchpilot promotes active zone assembly, Ca^{2+} channel clustering, and vesicle release. *Science*. 312:1051–1054.
6. Nagerl, U. V., K. I. Willig, B. Hein, S. W. Hell, and T. Bonhoeffer. 2008. Live-cell imaging of dendritic spines by STED microscopy. *Proc. Natl. Acad. Sci. USA*. 105:18982–18987.
7. Hein, B., K. I. Willig, and S. W. Hell. 2008. Stimulated emission depletion (STED) nanoscopy of a fluorescent protein-labeled organelle inside a living cell. *Proc. Natl. Acad. Sci. USA*. 105:14271–14276.
8. Hell, S. W. 2009. Microscopy and its focal switch. *Nat. Methods*. 6:24–32.
9. Denk, W., J. H. Strickler, and W. W. Webb. 1990. 2-Photon laser scanning fluorescence microscopy. *Science*. 248:73–76.
10. Moneron, G., and S. W. Hell. 2009. Opt. Express. 17:14567–14573.
11. Klar, T. A., and S. W. Hell. 1999. Subdiffraction resolution in far-field fluorescence microscopy. *Opt. Lett.* 24:954–956.
12. Westphal, V., and S. W. Hell. 2005. Nanoscale resolution in the focal plane of an optical microscope. *Phys. Rev. Lett.* 94:143903.
13. Torok, P., and P. R. T. Munro. 2004. The use of Gauss-Laguerre vector beams in STED microscopy. *Opt. Express*. 12:3605–3617.
14. Pawley, J. B., editor. 2006. Handbook of Biological Confocal Microscopy. Springer, New York.
15. Chalfie, M., Y. Tu, G. Euskirchen, W. W. Ward, and D. C. Prasher. 1994. Green fluorescent protein as a marker for gene expression. *Science*. 263:802–805.
16. Giepmans, B. N. G., S. R. Adams, M. H. Ellisman, and R. Y. Tsien. 2006. The fluorescent toolbox for assessing protein location and function. *Science*. 312:217–224.
17. Parton, R. G., and K. Simons. 2007. The multiple faces of caveolae. *Nat. Rev. Mol. Cell Biol.* 8:185–194.
18. Willig, K. I., R. R. Kellner, R. Medda, B. Hein, S. Jakobs, et al. 2006. Nanoscale resolution in GFP-based microscopy. *Nat. Methods*. 3: 721–723.
19. Tsien, R. Y. 1998. The green fluorescent protein. *Annu. Rev. Biochem.* 67:509–544.
20. Cormack, B. P., R. H. Valdivia, and S. Falkow. 1996. FACS-optimized mutants of the green fluorescent protein (GFP). *Gene*. 173:33–38.
21. Volkmer, A., V. Subramaniam, D. J. S. Birch, and T. M. Jovin. 2000. One- and two-photon excited fluorescence lifetimes and anisotropy decays of green fluorescent proteins. *Biophys. J.* 78:1589–1598.
22. Hosoi, H., S. Yamaguchi, H. Mizuno, A. Miyawaki, and T. Tahara. 2008. Hidden electronic excited state of enhanced green fluorescent protein. *J. Phys. Chem. B*. 112:2761–2763.
23. Hell, S. W., and J. Wichmann. 1994. Breaking the diffraction resolution limit by stimulated-emission: stimulated-emission-depletion fluorescence microscopy. *Opt. Lett.* 19:780–782.
24. Marsh, R. J., D. A. Armoogum, and A. J. Bain. 2002. Stimulated emission depletion of two-photon excited states. *Chem. Phys. Lett.* 366:398–405.
25. Mongin, O., L. Porres, L. Moreaux, J. Mertz, and M. Blanchard-Desce. 2002. Synthesis and photophysical properties of new conjugated fluorophores designed for two-photon-excited fluorescence. *Org. Lett.* 4: 719–722.
26. Bain, A. J., R. J. Marsh, D. A. Armoogum, O. Mongin, L. Porres, et al. 2003. Time-resolved stimulated emission depletion in two-photon excited states. *Biochem. Soc. Trans.* 31:1047–1051.
27. Klar, T. A., S. Jakobs, M. Dyba, A. Egner, and S. W. Hell. 2000. Fluorescence microscopy with diffraction resolution barrier broken by stimulated emission. *Proc. Natl. Acad. Sci. USA*. 97:8206–8210.
28. Westphal, V., S. O. Rizzoli, M. A. Lauterbach, D. Kamin, R. Jahn, et al. 2008. Video-rate far-field optical nanoscopy dissects synaptic vesicle movement. *Science*. 320:246–249.
29. Willig, K. I., J. Keller, M. Bossi, and S. W. Hell. 2006. STED microscopy resolves nanoparticle assemblies. *N. J. Phys.* 8:1–6.
30. Donnert, G., J. Keller, C. A. Wurm, S. O. Rizzoli, V. Westphal, et al. 2007. Two-color far-field fluorescence nanoscopy. *Biophys. J.* 92: L67–L69.
31. Wu, Q., F. Merchant, and K. Castleman. 2008. Microscope Image Processing. Academic Press, New York.
32. Tagawa, A., A. Mezzacasa, A. Hayer, A. Longatti, L. Pelkmans, et al. 2005. Assembly and trafficking of caveolar domains in the cell: caveolae as stable, cargo-triggered, vesicular transporters. *J. Cell Biol.* 170:769–779.
33. Campbell, L., A. J. Hollins, A. Al-Eid, G. R. Newman, C. von Ruhland, et al. 1999. Caveolin-1 expression and caveolae biogenesis during cell transdifferentiation in lung alveolar epithelial primary cultures. *Biochem. Biophys. Res. Commun.* 262:744–751.